International Journal of Nanoelectronics and Materials
Volume 13, No. 4, Oct 2020 [615-624]

Optical Properties of the Amine Functionalized Gold Nanobipyramids: Effect of Functionalization Times Period

Suratun Nafisah[1,2], Iwantono[1*], Marlia Morsin[2,3*], Yulia Citra[1], Sindi Melani[1] and Nur Liyana Razali[2,3]

[1]Department of Physics, Faculty of Mathematics and Natural Sciences, Universitas Riau, Kampus Bina Widya KM 12,5 Simpang Baru, Pekanbaru, 28293, Indonesia.
[2]Microelectronics & Nanotechnology – Shamsuddin Research Centre (MiNT-SRC), Institute of Integrated Engineering, Universiti Tun Hussein Onn Malaysia, 86400 Parit Raja, Batu Pahat Johor, Malaysia.
[3]Department of Electronic Engineering, Faculty of Electrical and Electronic Engineering, Universiti Tun Hussein Onn Malaysia, 86400 Parit Raja, Batu Pahat Johor, Malaysia.

Received 16 October 2019, Accepted 13 November 2020

ABSTRACT

The gold nanobipyramids (GNBPs) have attracted wide attention in field of sensing, biomedicine, catalysis and optoelectronics due to strong local electric field enhancement and surface plasmon resonance originated from their sharp tips. In GNBPs synthesis process, CTAB is usually used as a surfactant which plays a role as capping and stabilizing agents. However, CTAB surfactant is known as a toxic and thus hindering the GNBPs application in a biomedical related research. In this paper, for the first time we reported the simplest approach for surface modification of CTAB surfactant capped GNBPs using an amine functionalization or known as amine functionalized GNBPs. The optical properties and functionalization mechanism were investigated in this paper. In addition, the detailed understanding of the GNBPs-amine bond and its physical arrangement also were explained in this work. The amine functionalized GNBPs systems have exciting potential applications in the field of biosensing and in targeted drug delivery platforms.

Keywords: Amine Functionalization, Gold Nanobipyramids, Gold Nanoparticles, Localized Surface Plasmon Resonance (LSPR).

1. INTRODUCTION

Gold nanobipyramids (GNBPs) have been intensively studied because of their beneficial properties which have intensive local electric field enhancement and surface plasmon resonance larger than those of other elongated nanoparticles such as gold nanorods [1]. These properties make GNBPs have significant advantageous to be used in numerous applications such as in an immunosensor [2], LSPR sensor [3], colorimetric detection [4, 5], photothermal therapy [6], and laser [7, 8].

Thus far, the most convenient and prevailing way utilized to synthesis the GNBPs is using wet chemical approach namely seed-mediated growth method (SMGM). Using SMGM, more considerable efforts have been devoted to control their size, shape, density, and purity, which can immensely affect the properties of GNBPs, especially their optical properties [9–12]. In SMGM process commonly based on the reduction of $HAuCl_4$ by ascorbic acid as a reducing agent in the presence of growth directing surfactant, cetyltrimethylammoniumbromide (CTAB), which is usually employed to control the shape and size. Despite of that, the molecules of CTAB surfactant cause lower catalytic activity due to their micellular bilayer on the GNBPs surface

---

*Corresponding authors: *iwantono@lecturer.unri.ac.id*

that restricts the electron transfer and hinders the reactants to the active site [13, 14]. In addition, CTAB surfactant also known to be toxic and thus restricts applications of GNBPs in biomedical related research [15].

In order to outcome related issues, a great effort has been spent to removing, replacing or masking CTAB bilayer with non-toxic materials [14–16]. One of the approaches is through simple ligands exchange which known as a functionalization. Despite of their potential application in biomedical related research, the aggregation, dispersion, and control colloidal stability of GNBPs as well as manipulation their catalytic, optical, and electronic properties are some of the advantageous in functionalization of GNBPs [17]. Although various aromatic molecules such as amine [18], sulfonic [19], carboxyl group [20], or even phosphine moieties [21] have widely been used to functionalize gold nanoparticles, a little attention has been paid to the amine-functionalization of GNBPs until now. Hence, in this current study we have investigated the functionalization of GNBPs using amine ligand with emphasizes on effect of their optical properties.

2. MATERIAL AND METHODS

2.1 Reagents

Cetyltrimethylammonium bromide (CTAB), gold chloride, chloroplatinic acid, natrium borohydride, ascorbic acid, and (3-aminopropyl) trimethoxysilane (APTMS) were obtained from Sigma Aldrich. Silver nitrate was obtained from Honeywell Fluka. Hydrochloric acid (HCl) was obtained from RCI Labscan. All aqueous solutions of these chemicals were made using ultra-pure water with its resistivity of higher than 18.2 MΩ.

2.2 Preparation of Amine Functionalized Gold Nanobipyramids

GNBPs were synthesized using wet chemical method namely seed mediated growth method as reported in our previous works [1, 3]. The method was initially carried out by preparing two types of solutions namely as seed and growth solutions. The ca. 7 nm gold decahera seed solution was prepared by mixing 9.75 mL of 0.1 M CTAB, 0.15 mL of 0.01 M gold chloride, 0.1 mL of 0.01 M chloroplatinic acid, and 0.9 mL of 0.01 M ice-cold natrium borohydride. After storing for 2 h at temperature of 25 °C, 0.05 mL seed solution was added into growth solution that contained 20 mL of 0.1 M CTAB, 0.875 mL of 0.01 gold chloride, 0.025 mL of 0.01 M chloroplatinic acid, 0,2 mL of 0.01 M silver nitrate, 0.4 mL of 1 M hydrochloric acid, and 0.16 mL of 0.1 M ascorbic acid. After standing for 2 h at temperature of 25 °C, the GNBPs have grown. The functionalization of GNBPs with an amine was carried out by stirring the mixing solution containing 2 mL of 10 mM APTMS in ethanol and 20 mL of as-synthesized GNBPs solution at 500 rpm. The temperature during stirring was kept constant at 25 °C. The functionalization progress at certain time interval was observed by UV-Vis spectroscopy.

2.3 Instruments

UV-Vis spectra at wavelength from 400 nm to 1000 nm were characterized by a UV-1800 Shimadzu Spectrophotometer (Japan). The surface morphology of GNBPs was examined using Joel JSM-7600F field emission scanning electron microscopy (USA). HR-TEM image was acquired using Jeol JEM-ARM200F atomic resolution analytical microscopy (Japan). An X-ray diffraction (XRD) of GNBPs was analyzed using Bruker D8 Advance X-ray diffractometer (Germany) with diffraction angle ranges from 20° to 50°. For characterization, GNBPs solution was centrifuged for 30 min at 5000 rpm and then was dispersed in ultra-pure water. This process was repeated three times. Sample preparation for FESEM and XRD was carried out by deposited GNBPs on clean ITO and glass substrates, respectively. The sample was dried for 30 min in an oven with temperature of 50 ºC. Prior to HR-TEM characterization, the GNBPs were redispersed in 2-propanol and then dripped onto copper grids for image observation.

3. RESULTS AND DISCUSSION

A UV-Vis absorption spectrum of as-synthesized GNBPs (Figure 1) shows distinctly two localized surface plasmon resonance (LSPR) peaks appeared at the wavelength around 565 nm and 802 nm which corresponding to electron oscillation along transverse (t-SPR) and longitudinal (l-SPR) direction, respectively. Besides that, the peak shoulder arises from electron oscillation of nanosphericals which considered as by-product is also observed at the wavelength around 513 nm. The ratio of intensity between l-SPR and t-SPR bands was calculated from normalized absorbance to be 2.1:1. The peak intensity is related to the number of yield, and thus the obtained ratio of l-SPR and t-SPR peak intensity indicating relatively high yield of nanoparticles. Moreover, in this experiment, the FWHM value which derived from the spectrum of l-SPR peak was determined to be 126 nm, showing the size of GNBPs is almost uniform. The narrowness peak spectrum contributed to a good nanoparticles homogeneity.

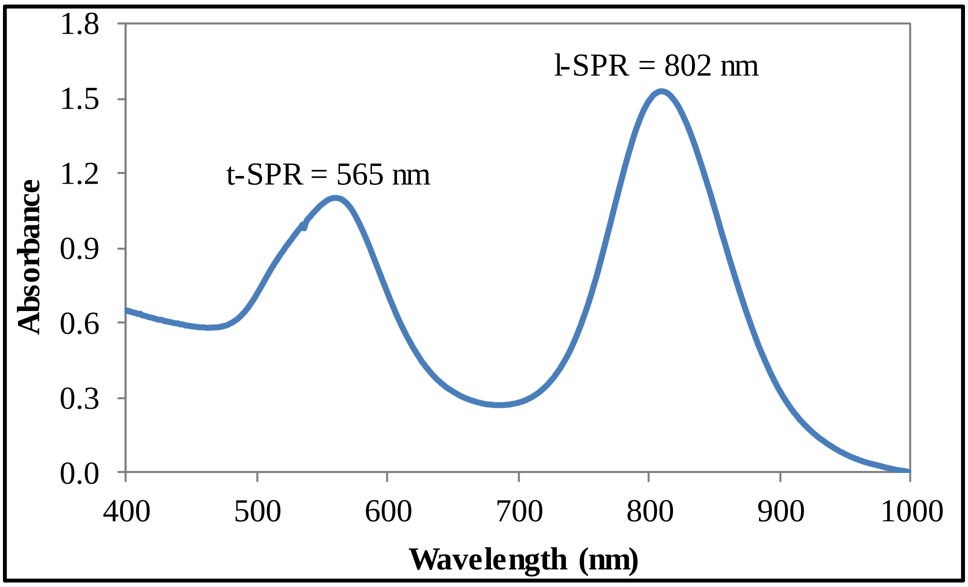

Figure 1. UV-Vis absorbance spectrum of GNBPs.

Field emission scanning electron microscopy (FESEM) image (Figure 2a) reveals the formation of high yield of GNBPs. The high resolution on transmission electron microscopy (HR-TEM) image was further verify the bipyramid-like nanostructure, which formed by two pyramids that share with the same base as it can be seen in Figure 2b. The size of GNBPs obtained from FESEM image is apparently uniform with the length and the diameter are 93.41±1.35 nm and 39.91±0.87 nm, respectively. The aspect ratio of GNBPs is 2.43±0.07. In addition, the yield percentage of GNBPs reaches up to 89.08±2.19 %.

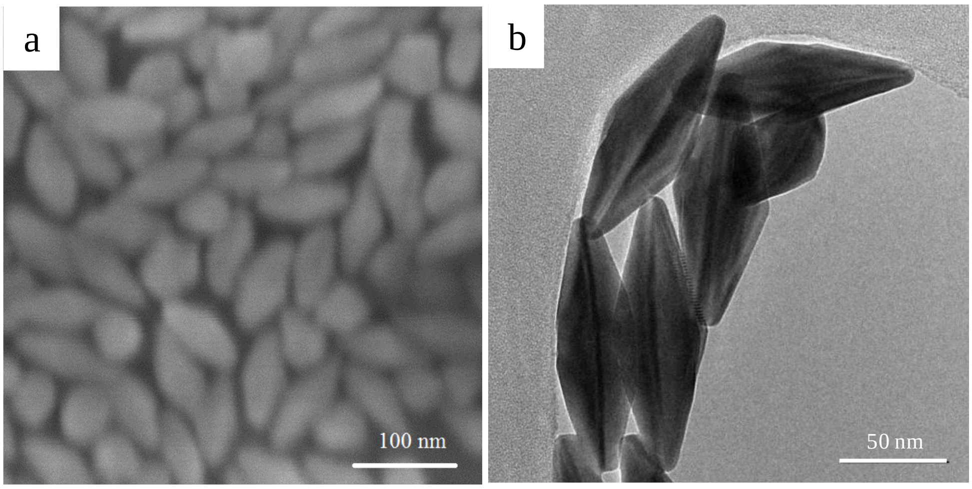

Figure 2. (a) FESEM and (b) HR-TEM image of GNBPs.

An X-ray diffraction (XRD) was employed to identify the crystallinity of the GNBPs. Figure 3 depicts the XRD pattern of GNBPs at the diffraction angle 2θ from 30° to 50°. The recorded XRD pattern exhibit two prominent diffraction peaks at 38.19° and 44.39° corresponding to (111) and (200) planes of Au with face centered cubic (FCC) crystalline structure. The lattice constant and crystallite size determined from XRD pattern are 4.08 Å and 23.64 nm, respectively. The results are in good agreement with the standard diffraction pattern of GNBPs reported by previous researchers [22, 23].

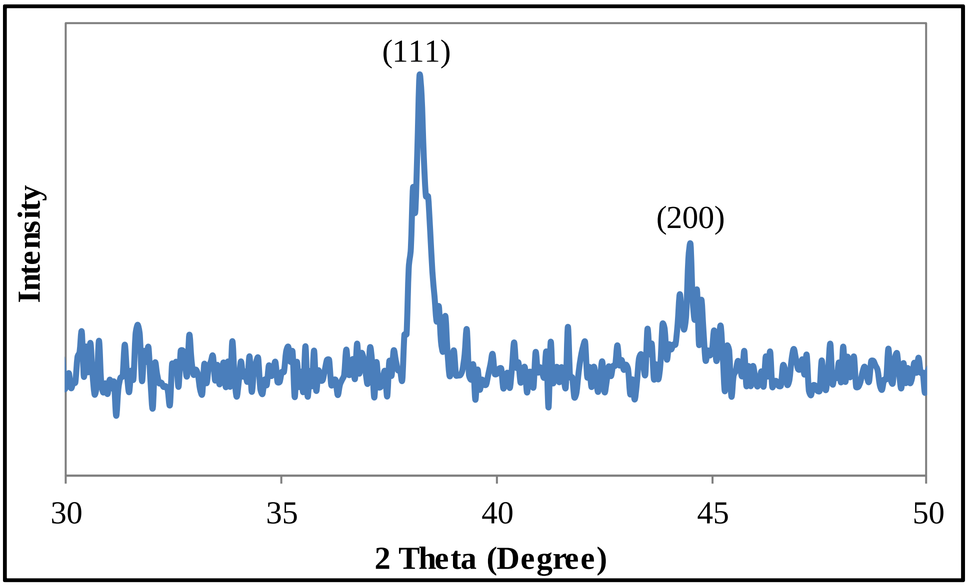

Figure 3. XRD pattern of GNBPs.

Then, the effects of functionalized amine with GNBPs were investigated. The functionalization of GNBPs with the amine was first examined by colour change of solution (Figure 4). After adding the amine for 4 h, the change in colour was observed from reddish (Figure 4a) to purple (Figure 4b). Moreover, the amine functionalized GNBPs at different functionalized time shows no vivid change in colour solution (Figure 4b-d).

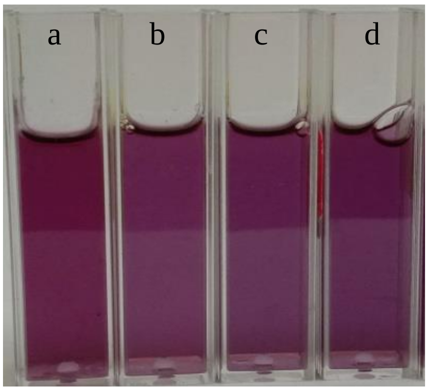

Figure 4. Colour of (a) GNBPs and (b-d) the amine functionalized GNBPs solution at functionalized times of (b) 4, (c) 12, and (d) 24 h.

The functionalization of GNBPs with the amine was further investigated by the UV-Vis measurement (Figure 5 and Table 1). As known, the LSPR of gold nanoparticles, especially GNBPs, very dependent to their morphological properties and easily influenced by their surrounding medium. As the functionalization reaction occurs, the plasmon peaks of GNBPs at a wavelength 565 nm for t-SPR and 802 nm for l-SPR gradually decrease to 547 nm and 794 nm, implying decreasing in GNBPs diameter and aspect ratio in this stage was occurred [24]. The reduction of GNBPs diameter was continuously occurred when functionalization time was extended to 12 h, however its aspect ratio increased as observed from its red-shifted of l-SPR peak which increased from 794 nm to 799 nm. When the functionalization time continuously extended up to 24 h, the diameter increased and thus decreasing its aspect ratio. The relationship between functionalization times versus LSPR peaks of the amine functionalized GNBPs was shown in Figure 6.

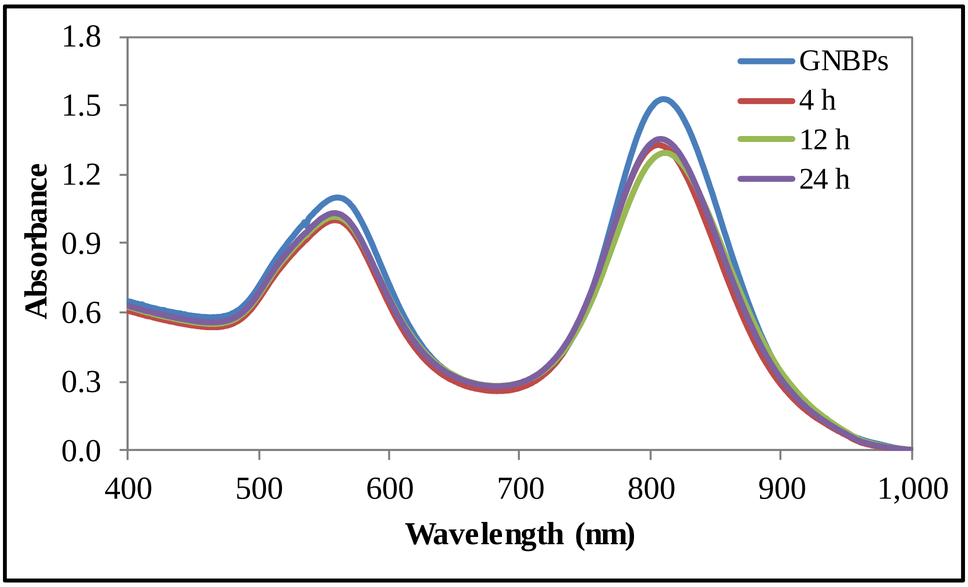

Figure 5. UV-Vis absorbance spectrum of GNBPs and the amine functionalized GNBPs at the various functionalization times.

Table 1 Optical parameters of the amine functionalized GNBPs at various functionalization times

Functionalization time (h)	t-SPR		l-SPR	
	Wavelength (nm)	**Absorbance (a.u)**	**Absorbance (a.u)**	**Wavelength (nm)**
0 (GNBPs)	565	1.168	802	1.503
4	547	0.974	794	1.281
12	543	0.973	799	1.252
24	548	1.013	793	1.287

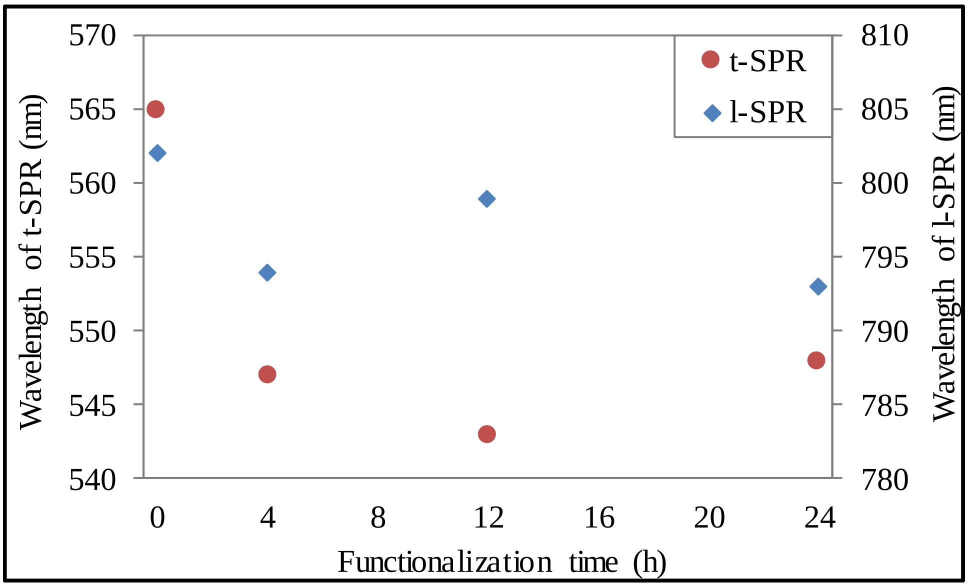

Figure 6. The LSPR wavelength peaks of the amine functionalized GNBPs with different functionalized times.

In addition, the optical parameter that can be observed from UV-Vis spectrum of the amine functionalized GNBPs is the peak intensity ratio between l-SPR and t-SPR. The peak intensity ratio is related to the percentage number of yield. The relationship of functionalization times versus l-SPR and t-SPR peak intensity ratio is plotted in Figure 7. The graph shows that percentage number of yield increases when GNBPs was functionalized with the amine and remain constant until the functionalization time of 12 h. For functionalization time of 24 h, the peak intensity ratio decreases. This decrement is suggesting due to the reverse reaction phenomenon which occurred after the system reach optimum condition (at functionalization time of 12 h). In reverse reaction, some of CTA$^+$ bilayers rebind on the GNBPs surface with higher surface energy and thus reduce the percentage number of yield [25].

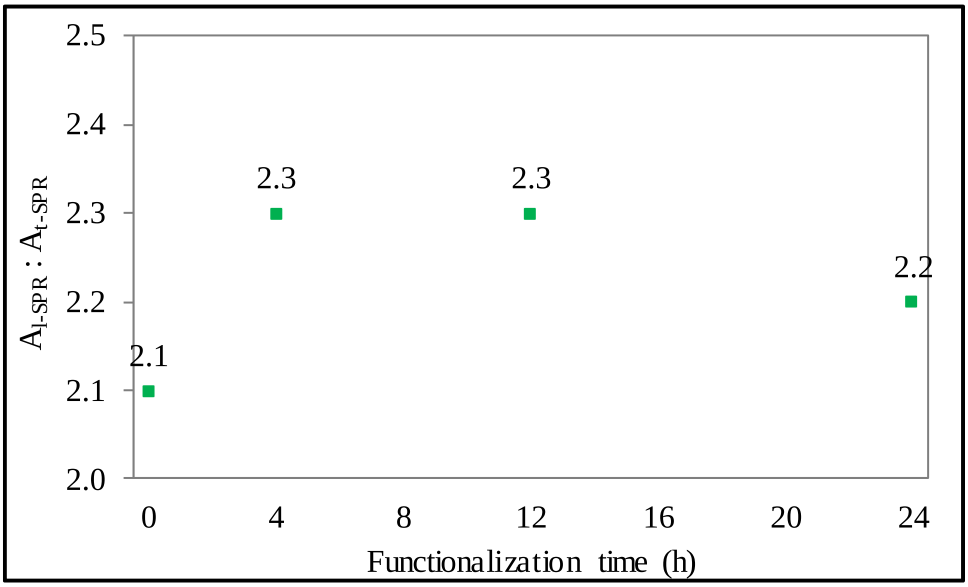

Figure 7. The ratio of intensity between l-SPR and t-SPR peaks of the amine functionalized GNBPs with different functionalized times.

From optical properties analysis, we propose the mechanism of functionalization of GNBPs with amine. At the initial stage, the surface of as-synthesized GNBPs was covered by capping agent (CTA^+) which originated from CTAB surfactant. This capping agent prevents GNBPs from agglomeration. In the second stage, the introduction of the amine molecules in the CTAB stabilized GNBPs system causes CTA^+ bilayer slowly release from GNBPs surface and replaces by the amine molecules [26]. The replacement of stabilizer agent from CTAB to the amine occurs due to the strong affinity of the amine molecules to gold surface which led the electrostatic attraction between gold surface and protonated amine [27]. This condition leads the reduction of both the GNBPs diameter and aspect ratio. When the functionalization time is extended until 12 h (third stage), the amine molecules have fully functionalized on GNBPs surface. Since the amine chain is shorter than CTA^+, the diameter of the amine functionalized GNBPs decrease and consequently reducing the size of aspect ratio. The functionalization times more than 12 h (fourth stage) leads the reversible reaction, indicated by some of CTA^+ self-assembled onto GNBPs with higher surface energy such as on its tips. The mechanism of the amine functionalized GNBPs is schematically shown in Figure 8.

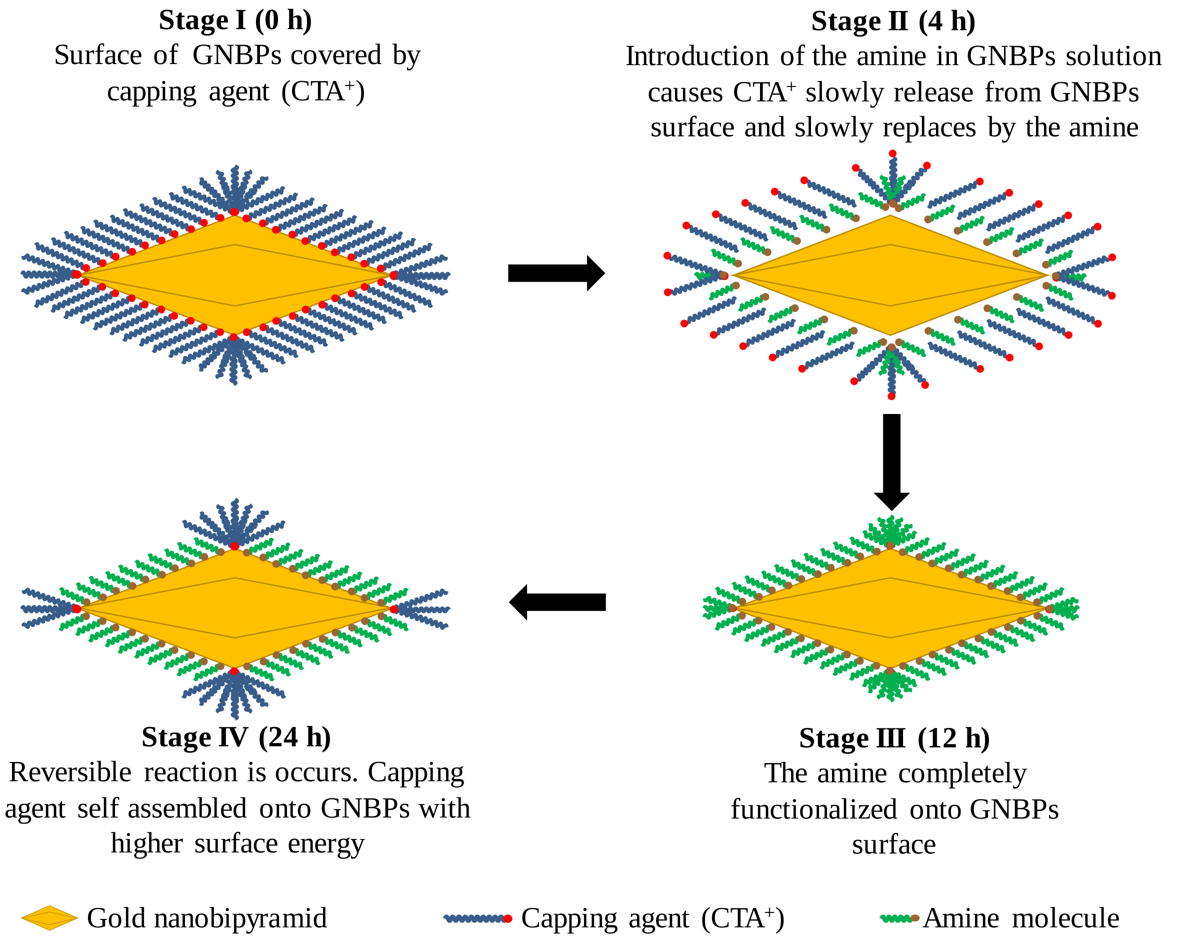

Figure 8. Mechanism of the amine functionalized GNBPs.

4. CONCLUSION

CTAB-stabilized GNBPs which known as toxic have been successfully functionalized with bio-inert and non-toxic amine through ligand exchange process. The morphological characterization depicts that as-synthesized GNBPs have length, diameter, and aspect ratio of 93.41±1.35 nm, 39.91±0.87 nm, and 2.43±0.07, respectively, while their yield percentage is 89.08±2.19 %. The functionalized nanoparticles which exhibit unique optical spectroscopic was investigated using UV-Vis spectrometry. Significantly, it was observed that at the first stage of functionalization process, the GNBPs plasmon resonances are red-shifted. The complete functionalization process was occurred for functionalization time of 12 h. The presented method is efficacious for wide range application of GNBPs especially in biomedical related research.

ACKNOWLEDGEMENTS

This research was financially supported by Kementerian Riset dan Teknologi / Badan Riset dan Inovasi Nasional Republik Indonesia through Skema Penelitian Pascasarjana No. 457/UN.19.5.1.3/PT.01.03/2020. Author's extended gratitude to Microelectronics & Nanotechnology - Shamsuddin Research Centre (MiNT-SRC) for the laboratory facilities.

REFERENCES

[1] Nafisah, S., Morsin, M., Sanudin, R., Nayan, N., Mohd Yusop, M. Z., Razali, N. L., Md Shah, M. Z. A., J. Phys. Chem. Solids **In Press** (2020).

[2] Huynh, T. P., Ngo, V. K. T., Nguyen, D. G., Nguyen, H. P. U., Nghiem, Q. D., Lam, Q. V., Huynh, T. D., J. Electron. Mater. **45**, 5 (2016) 2516–2521.

[3] Nafisah, S., Morsin, M., Jumadi, N. A., Nayan, N., Mohd Shah, N. S., Razali, N. L., An'Nisa, N. Z., IEEE Sens. J. **20**, 5 (20202378–2389.

[4] Xu, S., Ouyang, W., Xie, P., Lin, Y., Qiu, B., Lin, Z., Chen, G., Guo, L., Anal. Chem. **89**, 3 (2017) 1617–1623.

[5] Xu, S. Jiang, L., Liu, Y., Liu, P., Wang, W., Luo, X., Anal. Chim. Acta **1071** (2019) 53–58.

[6] Feng, J., Chen, L., Xia, Y., Xing, J., Li, Z., Qian, Q., Wang, Y., Wu, A., Zeng, L., Zhou, Y., ACS Biomater. Sci. Eng. **3**, 4 (2017) 608–618,.

[7] Zhang, H., Liu, J., Opt. Lett. **41**, 6 (2016) 1150–1152.

[8] Zhang, W., Zhang, H., Feng, G., Ju, Y., Ning, S., Chen, X., Dai, J., Zhou, S., Opt. Laser Technol. **111** (2019) 30–34.

[9] Bandyopadhyay, S., Singh, G., Glomm, W. R., Mater. Today Chem. **3** (2017) 1–9.

[10] Torresan, M. F., Angelomé, P. C., Bazán-Díaz, L., Velázquez-Salazar, J. J., Mendoza-Cruz, R., Iglesias, R. A., José-Yacamán, M., Nanotechnology **30**, 20 (2019) 1–12.

[11] Yip, H. K., Zhu, X., Zhuo, X., Jiang, R., Yang, Z., Wang, J., Adv. Opt. Mater. **5**, 24 (2017) 1–13.

[12] Li, Q., Zhuo, X., Li, S., Ruan, Q., Xu, Q. H., Wang, J., Adv. Opt. Mater. **3**, 6 (2015) 801–812.

[13] Park J. W., Shumaker-Parry J. S., ACS Nano **9**, 2 (2015) 1665–1682.

[14] Zheng, B., Liu, X., Wu, Y., Yan, L., Du, J., Dai, J., Xiong, Q., Guo, Y., Xiao, D., Inorg. Chem. Front. **4**, 8 (2017) 1268–1272.

[15] Allen, J. M., Xu, J., Blahove, M., Canonico-May, S. A., Santaloci, T. J., Braselton, M. E., Stone, J. W., J. Colloid Interface Sci. **505** (2017) 1172–1176.

[16] Alex, S., Tiwari, A., J. Nanosci. Nanotechnol. **15**, 3 (2015) 1869–1894.

[17] Gao, X., Xu, G., Yan, Z., Li, S., Shi, F., Chen, Y., RSC Adv. **5**, 107 (2015) 88045–88051.

[18] Shikha, S., Thakur, K. G., Bhattacharyya, M. S., RSC Adv. **7**, 68 (2017) 42845–42855.

[19] Liang, Z., Zhai, H., Chen, Z., Wang, H., Wang, S., Zhou, Q., Huang, X., Sensors Actuators B Chem. **224** (2016) 915–925.

[20] Pellegrino, S., Bonetti, A., Clerici, F., Contini, A., Moretto, A., Soave, R., Gelmi, M. L., J. Org. Chem. **80**, 11 (2015) 5507–5516.

[21] Zong, J., Cobb, S. L., Cameron, N. R., Biomater. Sci. **5**, 5 (2017) 872–886.

[22] Ngo, V. K. T., Huynh, T. P., Nguyen, D. G., Nguyen, H. P. U., Lam, Q. V., and Huynh, T. D., Adv. Nat. Sci. Nanosci. Nanotechnol. **6**, 4 (2015) 45017.

[23] Fang, C., Zhao, G., Xiao, Y., Zhao, J., Zhang, Z., Geng, B., Nat. Sci. Rep. **6** (2016) 1–8.

[24] Moores, A., Goettmann, F., New J. Chem. **30**, 8 (2006) 1121–1132.

[25] Gao, H. M., Liu, H., Qian, H. J., Jiao, G. S., Lu, Z. Y., Phys. Chem. Chem. Phys. **20**, 3 (2018) 1381–1394.

[26] Zhang, Z., Ross, R. D., Roeder, R. K., Nanoscale **2**, 4 (2010) 582–586.

[27] Harish, S., Sabarinathan, R., Joseph, J., Phani, K. L. N., Mater. Chem. Phys. **127** (2011) 203–207.